# High Density Shapes Using Photometric Stereo and Laser Range Sensor under Unknown Light-Source Direction

Tomoyuki Kamikawa, Daisuke Miyazaki, Masashi Baba, Ryo Furukawa,
Masahito Aoyama, Shinsaku Hiura, and Naoki Asada
Hiroshima City University
Hiroshima, JAPAN
http://ime.info.hiroshima-cu.ac.jp/

## Abstract

*Much research is in progress on the acquisition of high-density three-dimensional shapes by acquiring and combining shape data and normal data. The method proposed in this paper estimates normals to object surfaces by employing the photometric stereo method and combines the estimation with the three-dimensional shape acquired by a laser range sensor. Although the photometric stereo method presumes that light-source directions for each image are known, the proposed method uses its light-source direction estimates. By linearizing the images as preprocessing, specular reflection and shadow effects within the image are removed and the precision for the light-source direction estimations is increased. Since the proposed method does not require the light-source directions to be known, it offers the advantage of broad applicability for measurement work.*

## 1 Introduction

Three-dimensional (3D) modeling technologies of physical objects constitute vital technologies that are employed for a number of purposes, including digital archiving and works of fine art, and constructing realistic virtual spaces. One method to create 3D models is to use a dedicated measuring device such as a laser range sensor. This method, however, cannot determine the surface shaping of the object for a detailed mesostructure. Consequently, research is in progress to create high-density 3D models by estimating and combining shape data and normal data.

The photometric stereo method estimates normals from the change in brightness across multiple images obtained by varying the light-source direction [1]. Use of the photometric stereo method, however, is restricted to a known light-source direction and perfectly diffuse reflection of the object's surfaces. Furthermore, reconstruction of the 3D shape proceeds by integral calculus of estimated normals. Adjacent pixels accumulate errors that become quite large overall.

Our research attempts to estimate normals of high density in an environment where the light-source direction is unknown. The method employed uses the 3D shape obtained by a laser range sensor and multiple images obtained by altering the light-source direction. First, image linearization is conducted as preprocessing. Image linearization means to remove specular reflection and shadow effects and to convert an image of solely diffuse reflection components. This work was necessary, because the photometric stereo method assumes that no specular reflection or shadow exists.

By using the 3D shape obtained from the laser range sensor and multiple images, the light-source directions were estimated. The photometric stereo method was applied with the estimated light-source directions, and normals were estimated. Mapping these normals to the 3D shape obtained with the laser range sensor enabled the acquisition of a high-density 3D shape more detailed than that by using just the laser range sensor. Our method achieved the acquisition of a high-density 3D shape by mutually compensating between the drawbacks of the laser range sensor and those of the photometric stereo method. At the end of this paper, we show a shape estimation result with reproducing small-scale details, which will be useful in many application fields.

## 2 Related Work

As described above, research concerning the creation of high-density 3D models by estimating shape data and normal data and combining them is progressing. Nehab et al. [2] proposed a method of acquiring high-precision shape data by combining the 3D shape acquired by a laser range sensor and normals estimated by the photometric stereo method. Later their method is improved by Okatani et al. [3] which produces more precise shape. Ochiai et al. [4] mapped the surface normal obtained by photometric stereo onto the 3D shape obtained by laser range sensor. Inspired by above research, we also combine the surface normal obtained by photometric stereo and the 3D geometry obtained by laser range sensor.

For preprocessing, image linearization is useful for applying photometric stereo. Mori et al. [5] employed an image linearization method in which photometric phenomena were classified in principal component analysis. Mukaigawa et al. [6] proposed a RANSAC-based method for image linearization, while Miyazaki and Ikeuchi [7] iteratively computed the singular value decomposition in order to linearize the image. We use Mori's method [5] for image linearization. Unlike their method, we also consider the penumbra in our linearization method.

Light-source direction can be estimated using the shape obtained by laser range sensor or other sensors. Tachikawa et al. [8] proposed light-source direction estimation from two images under different lighting conditions of a known object. Unten and Ikeuchi [9] estimated the light-source direction by representing a set of light sources surrounding the object spherically. Du et al. [10] estimated the light-source direction which is represented by spherical harmonics. We use Tachikawa's method [8] for light-source direction

estimation. Unlike their method, we use RANSAC approach for robustly estimate the light source direction. They applied their method to two input images, while we apply our method to more than two input images.

## 3 Image Linearization According to Photometric Phenomena Classification

The process of removing specular reflection and shadows and converting the image to one of solely diffuse reflection is called image linearization. This section describes the method of conducting image linearization according to classification of photometric phenomena.

### 3.1 Image Linearization

According to Shashua [11], by assuming a parallel light source and a perfectly diffuse reflective surface, a linear combination of three basis images of differing light-source directions can express an image of arbitrary light-source direction. When the three basis images are $\hat{I}_1$, $\hat{I}_2$, and $\hat{I}_3$ (the orthonormal basis), the image $I_k^L$ of the arbitrary light-source direction can be expressed by the following linear combination.

$$
\begin{aligned}
A^L &= \hat{A}C, \quad (1)\\
A^L &= (I_1^L, I_2^L, \cdots, I_m^L),\\
\hat{A} &= (\hat{I}_1, \hat{I}_2, \hat{I}_3),\\
C &= (C_1, C_2, \cdots, C_m),\\
C_k &= (\alpha_k, \beta_k, \gamma_k)^\top.
\end{aligned}
$$

The actual image contains shadows and specular reflection, and therefore does not satisfy Equation (1). Linearization coverts an image to one with solely diffuse reflection to satisfy Equation (1).

### 3.2 Classification of Photometric Phenomena

Comparison of input images and their linearized images enables classification of pixels into five types: diffuse reflection, specular reflection, attached shadow, cast shadow, and penumbra. These classifications are based on the following properties of photometric phenomena. As shown in Figure 1, photometric phenomena is classified by establishing threshold values $T_{sp1}$, $T_{sp2}$, $T_{p1}$, and $T_{p2}$. See Mori et al. [5] for more details, though we introduce penumbra class which is not introduced in their method.

### 3.3 Linearization Steps

The following describes the image linearization procedures.

(a) **Acquisition of input image sequence**
Positions of the camera and object of interest are fixed. Multiple images photographed under varied light-source direction are inputs. The light-source direction, 3D shape, and reflectance of the scene of interest may be unknown.

(b) **Computation of basis image** Basis image sequence matrix $\hat{A}$ and coefficient set $C$ are computed by principal component analysis from the input image sequence matrix $A^L$.
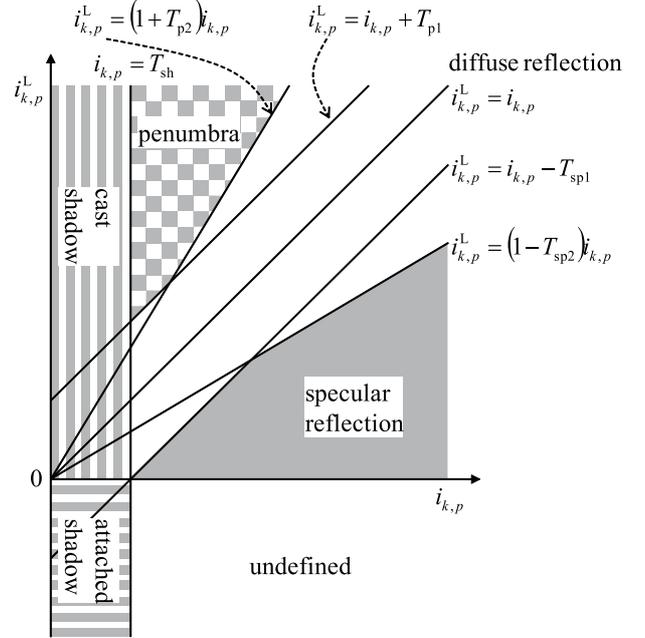


Figure 1. Classification criteria of photometric phenomena

(c) **Computation of linearized images** The input image sequence is linearized by calculating the dot product of the basis image sequence matrix $\hat{A}$ and coefficient set $C$.

(d) **Classification of photometric phenomena** Pixel values $i_{k,p}$ of the input images and pixel values $i_{k,p}^L$ of the linearized images are compared, and the photometric phenomena at each pixel are classified (see Section 3.2).

(e) **Denoising by embedding** Pixel values of linearized images are embedded to pixels of input images classified as specular reflection, attached shadow, cast shadow, and penumbra.

(f) **Making threshold values more rigorous** Steps (b) to (e) of the procedure are iterated by using the input image sequence updated with the embedded pixel values. In the iteration process, threshold values $T_{sp1}$, $T_{sp2}$, $T_{p1}$, and $T_{p2}$ are made slightly smaller.

(g) **Output of linearized images** When the iteration-terminating condition established in step (f) is satisfied, linearized images $A^L$ are output.

## 4 Estimation of Light-Source Direction by Observing Object of Known Shape

This section describes the method for estimating the light-source direction. The method in this section uses two images as inputs. When estimating light-source directions for each image, an image pair with a large overlap in the brightest portions for each image was selected, and light-source directions were estimated together for the pair images.

## 4.1 Acquistion of Light-Source Direction

The normal vector $N_p$ of point $P$, the light source vectors $L_1$ and $L_2$ when photographing image 1 and image 2, respectively, and the radiance $I_{1p}$ and $I_{2p}$ when photographing image 1 and image 2, respectively, are related with the following equation (Tachikawa et al. [8]).

$$
\begin{aligned}
ML' &= 0 \qquad\qquad\qquad\qquad\qquad (2)\\
M &= (m_1, m_2, \cdots, m_q)^\top,\\
L' &= (L_{1x}, L_{1y}, L_{1z}, L_{2x}, L_{2y}, L_{2z})^\top,\\
m_p &= (I_{2p}N_{px}, I_{2p}N_{py}, I_{2p}N_{pz},\\
&\quad\ -I_{1p}N_{px}, -I_{1p}N_{py}, -I_{1p}N_{pz})^\top,\\
L_1 &= (L_{1x}, L_{1y}, L_{1z})^\top,\\
L_2 &= (L_{2x}, L_{2y}, L_{2z})^\top,\\
N_p &= (N_{px}, N_{py}, N_{pz})^\top.
\end{aligned}
$$

Since the rank for matrix $M$ is 5, $L'$ can be derived as the sixth right-singular vector upon singular value decomposition of matrix $M$.

## 4.2 Robust Framework for Estimating Light-Source Direction

Under the premise that the laser range sensor could not measure the detailed mesostructure of the object surface, robust estimation was considered effective for removing errors emerging in portions that could not be measured. This research employed RANSAC to conduct robust estimation according to the following procedure:

(1) From all points $m_1, \cdots, m_q$, $R$ points are randomly selected.

(2) Matrix $M$ is created from the $R$ points selected, and $L'$ is determined according to the method in Section 4.1.

(3) For all points $m_1, \cdots, m_q$, the derived $L'$ component is used to determine the left-hand side $m_p^\top L'$ of Equation (2), using $\|m_p^\top L' - 0\|$ as an error metric.

(4) The number of points whose errors are within threshold value $T$ is counted.

(5) The trial of Steps (1) to (4) is iterated, and $L'$ with the largest number of points whose errors are within the threshold value is set as the provisional parameter.

The provisional parameter $L'$ determined according to the above procedure was used to determine the error metric $\|m_p^\top L' - 0\|$ again. Only the points whose errors were within the threshold value were selected to create matrix $M$, and $L'$ was again determined by the method in Section 4.1. The newly derived $L'$ was adopted as the final estimated light-source vector.



(a) (b)

Figure 2. One of the images: (a) Input image. (b) An image linearized by our method, where red pixels represent the negative intensity.



estimated light
true light
(a) (b)
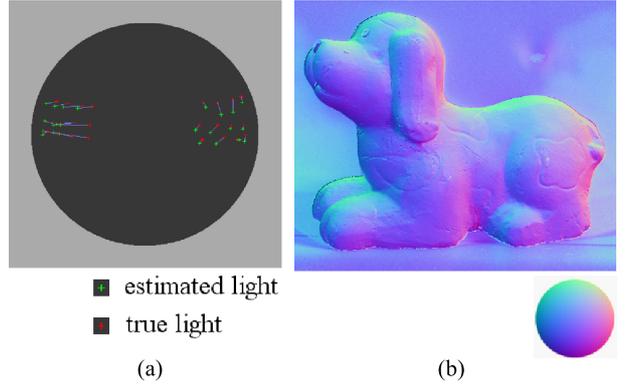
Figure 3. Estimated values: (a) Estimated light-source direction. (b) Estimated normals.

## 5 Experiment

This section describes the experimental results of data acquired from shape measurements and image photography of actual objects. The Konica-Minolta VIVID910 was employed for shape measurements, and the Apogee Alta U16000C for image photography. The data used for input are shown in Figure 2 (a). The number of images used was 24. Linearized image is shown in Figure 2 (b).

The results of estimating the light source direction are shown in Figure 3 (a). To evaluate the estimation error, true light source direction are obtained from a metal sphere. In Figure 3 (a), the light-source directions of all input images are plotted on a single image, where the true values are red and the estimated values are green. The average error established as the angle between the estimated value and the true value of a light-source direction vector was 8.063 degrees.

The normals estimated according to the photometric stereo method using the light-source directions determined in the previous step are shown in Figure 3 (b). The lower right sphere of Figure 3 (b) presents the correspondence between normal vectors and RGB color coding.

The results of normal mapping to the input shape (Figure 4 (a)) with the estimated normals (Figure 3 (b)) are shown in Figure 4 (b). Reconstruction of the detailed shape, such as the surface patterns and
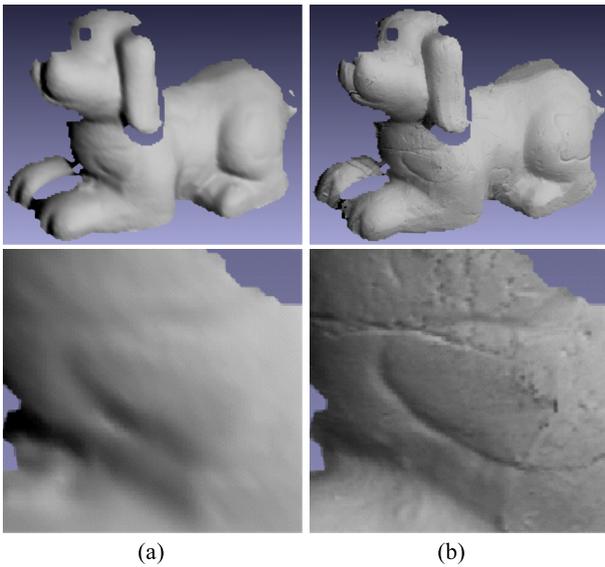
Figure 4. Result: (a) Shape obtained by laser range sensor. (b) Normal mapping result obtained by our method.

scratches, which could not be obtained by the shape measurement device alone, was confirmed.

## 6 Conclusion

This paper proposed a method for acquiring high-density 3D shapes by employing the photometric stereo method, even though the light-source direction is unknown. The proposed method was confirmed as being capable of reconstructing the detailed mesostructure that could not be obtained by a laser range sensor alone. By conducting preliminary image linearization, subsequent light-source direction and normal estimation can be expected to retain high precision compared to other methods using images without performing linearization. This method also imposes a smaller burden on actual measurement work, since the light-source direction does not need to be known. In this context, the proposed method offers broad applicability.

## References

[1] R. J. Woodham, "Photometric method for determining surface orientation from multiple images," *Optical Engineering*, vol. 19, no. 1, pp. 139–144, 1980.

[2] D. Nehab, S. Rusinkiewicz, J. Davis, and R. Ramamoorthi, "Efficiently combining positions and normals for precise 3D geometry," *ACM Trans. Graph.*, vol. 24, no. 3, pp. 536–543, 2005.

[3] T. Okatani and K. Deguchi, "Optimal integration of photometric and geometric surface measurements using inaccurate reflectance/illumination knowledge," in *Proceedings on IEEE Computer Society Conference on Computer Vision and Pattern Recognition*, 2012.

[4] K. Ochiai, N. Tsumura, T. Nakaguchi, K. Miyata, and Y. Miyake, "Gonio-spectral based digital archiving and reproduction system for electronic museum," *ACM SIGGRAPH 2006 Research posters*, Article 97, 2006.

[5] T. Mori, S. Hiura, and K. Sato, "Shadow and specular removal by photometric linearization based on PCA with outlier exclusion", in *Proceedings on International Conference on Computer Vision Theory and Applications*, pp. 221–229, 2012.

[6] Y. Mukaigawa, Y. Ishii, and T. Shakunaga, "Analysis of photometric factors based on photometric linearization," *J. Opt. Soc. Am. A*, vol. 24, no. 10, pp. 3326–3334, 2007.

[7] D. Miyazaki and K. Ikeuchi, "Photometric stereo under unknown light sources using robust SVD with missing data," in *Proceedings on IEEE International Conference on Image Processing*, pp. 4057–4060, 2010.

[8] T. Tachikawa, S. Hiura, and K. Sato, "Robust estimation of light directions and albedo map of an object of known shape", *IPSJ Transactions on Computer Vision and Applications*, vol. 3, pp. 172–185, 2011.

[9] H. Unten and K. Ikeuchi, "Color alignment in texture mapping of images under point light source and general lighting condition," in *Proceedings on IEEE Computer Society Conference on Computer Vision and Pattern Recognition*, vol. 1, pp. 234–239, 2004.

[10] F. Du, T. Okabe, Y. Sato, and A. Sugimoto, "Reflectance estimation from motion under complex illumination," in *Proceedings on International Conference on Pattern Recognition*, vol. 3, pp. 218–222, 2004.

[11] A. Shashua, "Geometry and photometry in 3D visual recognition," *Ph.D thesis, Dept. Brain and Cognitive Science, MIT*, 1992.